

Magnetic excitations and exchange interactions in the spin- $\frac{1}{2}$ two-leg ladder compound $\text{La}_6\text{Ca}_8\text{Cu}_{24}\text{O}_{41}$

M. Matsuda* and K. Katsumata

RIKEN (The Institute of Physical and Chemical Research), Wako, Saitama 351-0198, Japan

R. S. Eccleston

ISIS Facility, Rutherford Appleton Laboratory, Chilton, Didcot, Oxfordshire OX11 0QX, United Kingdom

S. Brehmer and H.-J. Mikeska

Institut für Theoretische Physik, Universität Hannover, D-30167 Hannover, Germany

(Received 21 April 2000)

Using a pulsed neutron source we have been able to observe inelastic signals at high energies from the ladders of $\text{La}_6\text{Ca}_8\text{Cu}_{24}\text{O}_{41}$. These signals constitute the magnon branch ($\sim 30 \leq E \leq \sim 190$ meV) for the lowest triplet excitation. A fit to a theory including a coupling along the leg (J_{leg}) and rung (J_{rung}) alone gives the value $J_{\text{leg}}/J_{\text{rung}} \sim 2$ that is not consistent with expectations from a geometrical consideration and the exact diagonalization calculation. This inconsistency is removed when our data are fitted with $J_{\text{leg}} = J_{\text{rung}} = 110$ meV and a four-spin exchange interaction, $J_{\text{ring}} = 16.5$ meV.

I. INTRODUCTION

Quantum antiferromagnetism in lower dimensions has attracted much attention from condensed-matter physicists. In recent years, spin-ladder systems have been the subject of intense theoretical and experimental studies.¹ A spin ladder is composed of n coupled one-dimensional magnets with an interchain (or rung) interaction J_{\perp} (J_{rung}). The most extensively studied spin-ladder system is the one in which the magnetic atoms have spin quantum number (S) $\frac{1}{2}$ with an antiferromagnetic intrachain (or leg) interaction J_{\parallel} (J_{leg}) as well as an antiferromagnetic J_{\perp} . The magnetic properties of such $S = \frac{1}{2}$ antiferromagnetic ladders (AFL's) change radically depending on whether n is even or odd.^{2,3} The ground state of an $S = \frac{1}{2}$ AFL with even n is a singlet with a short spin-spin correlation length and an energy gap to the lowest excited triplet. On the other hand, an $S = \frac{1}{2}$ AFL with odd n has no gap in the excitation spectrum and the spin-spin correlation decays as a power law.

The existence of an energy gap in the excitation spectrum of an $S = \frac{1}{2}$ two-leg AFL can be understood intuitively as follows. When $J_{\perp} \gg J_{\parallel}$ (> 0), the system is viewed as a collection of almost independent $S = \frac{1}{2}$ dimers. In this case, the low-energy spectrum consists of a singlet ground state and an excited triplet with an energy gap of J_{\perp} . Theoretical studies⁴⁻⁸ showed that on decreasing J_{\perp} the energy gap decreases and the triplet excitation has a dispersion. The excitation energy is minimum at wave vector (Q) equals to π . The energy gap (spin gap) at $Q = \pi$ is given by $0.504J_{\perp}$ for an isotropic ($J_{\perp} = J_{\parallel}$) two-leg ladder.⁹ Despite this progress in theoretical studies, little is known experimentally about the low-energy excitation spectrum of a spin ladder. In this paper, we report the observation of a dispersion curve for the low-energy excitation in a spin-ladder material.

The compound chosen for this study is $\text{La}_6\text{Ca}_8\text{Cu}_{24}\text{O}_{41}$. The parent compound $\text{Sr}_{14}\text{Cu}_{24}\text{O}_{41}$ consists of both CuO_2

chains and Cu_2O_3 ladders of copper ions^{10,11} as shown in Fig. 1. The Cu_2O_3 ladder is a good realization of an $S = \frac{1}{2}$ Heisenberg two-leg ladder. As shown in Fig. 1(b), the copper moments are coupled by almost 180° Cu-O-Cu bonds along the a and c axes. The neighboring ladders are coupled by almost 90° Cu-O-Cu bonds which give a ferromagnetic interaction. Because this ferromagnetic interaction is much weaker than the dominant antiferromagnetic interaction together with a frustration that occurs between the two interactions, these ladders are almost decoupled.⁵ A number of experiments showed that the two-leg ladder has a spin gap of $28 - 56$ meV.¹²⁻¹⁶ An important point in the $\text{Sr}_{14}\text{Cu}_{24}\text{O}_{41}$ system is that stoichiometric $\text{Sr}_{14}\text{Cu}_{24}\text{O}_{41}$ contains hole carriers. It has been reported that most of the holes are localized in the chain and some exist in the ladder.¹⁷⁻²⁰ When Sr^{2+} sites are substituted by Ca^{2+} ions, the total number of holes in the sample is unchanged but holes are transferred from the chain to the ladder.^{19,20} These holes in the ladder may broaden the excitation spectrum and make the observation difficult. On the contrary, the compound $\text{La}_6\text{Ca}_8\text{Cu}_{24}\text{O}_{41}$ has no holes either in the chain or in the ladder, therefore, we

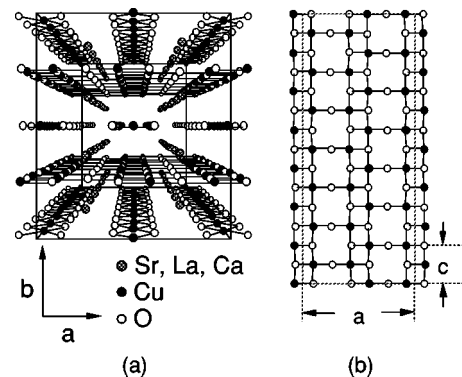


FIG. 1. Structure of (a) the $\text{Sr}_{14}\text{Cu}_{24}\text{O}_{41}$ system viewed from the c axis and (b) the Cu_2O_3 ladder layer.

expect that a cleaner spectrum will be observed in this compound.

II. EXPERIMENTAL DETAILS

The single crystals of $\text{La}_6\text{Ca}_8\text{Cu}_{24}\text{O}_{41}$ were grown using a traveling solvent floating-zone (TSFZ) method at 3 bars oxygen atmosphere. An array of four mutually aligned single crystals was used. The dimension of the cylindrically shaped crystals is about $5 \times 5 \times 40 \text{ mm}^3$. The neutron-scattering experiments were carried out on the High Energy Transfer (HET) Chopper Spectrometer on the ISIS Pulsed Neutron Source at the Rutherford Appleton Laboratory. The experiments were carried out with incident neutron energies of 150, 300, 500, and 600 meV that were monochromated by a rotating Fermi chopper that was phased to the source. The energy resolution at $\Delta E=0$ meV is 6.2, 12, 24.8, and 32 meV for $E_i=150, 300, 500,$ and 600 meV, respectively. The single crystals were mounted on a closed-cycle refrigerator. The experiments were performed with two configurations; incident beam parallel to a (the rung direction) or c axes (the leg direction). Since the chains in $\text{La}_6\text{Ca}_8\text{Cu}_{24}\text{O}_{41}$ show long-range antiferromagnetic ordering below 12.2 K,^{17,21} all the measurements were performed at 20 K where the magnetic properties in the ladder are not affected by staggered magnetic fields from the chain.

III. EXPERIMENTAL RESULTS AND DISCUSSION

A. Inelastic neutron-scattering experiments

Figure 2 shows the inelastic neutron spectra in $\text{La}_6\text{Ca}_8\text{Cu}_{24}\text{O}_{41}$ at 20 K with incident beam ($E_i=300, 500,$ and 600 meV) parallel to the c axis. The filled circles represent the raw spectra. The inset shows the scan loci in energy versus Q ($\omega-Q$) space. Several inelastic peaks are observed. The signal originates from both magnetic excitations and a background contribution. The majority of the background signal is multiple phonon scattering in the sample, with a smaller single phonon scattering contribution and a small contribution from the Al sample cell and the heat shields of the closed-cycle refrigerator.

The scattering function of a spin ladder along the a direction (i.e., perpendicular to the ladder direction and in the case of these data the incident beam direction) is sinusoidal, being zero at $k_a=0$ and a maximum at $k_a=0.8 \text{ \AA}^{-1}$ corresponding to the length of a rung. Consequently we expect to see magnetic scattering from the ladder in the $a-c$ plane, but not in the $b-c$ plane. With the crystal aligned as it was for our experiment, detectors in the horizontal plane probe the $a-c$ plane whereas those in the vertical plane probe the $b-c$ plane. As a result we were able to use the vertical detector bank to simultaneously collect the background scattering data under identical experimental conditions. Although the vertical detectors are probing a different portion of reciprocal space, the multiphonon background is isotropic to a good approximation at the high energies at which we have measured. The open circles in Fig. 2 represent the background signal. As an additional check of our estimates of the background subtraction, we performed scans with k_i perpendicular to the c axis that once again means that there is no magnetic signal in the vertical detector banks. Even from the raw

data in Fig. 2, one can see the magnetic peaks. The open triangles represent the inelastic spectra after subtracting the background. The broken curves in Fig. 2 are the results of fits to a convolution of the resolution function with Gaussians.

As will be described in Sec. III C, the minimum and maximum of the triplet excitation band should be known to determine the exchange constants in the Cu_2O_3 ladder. In order to determine these values, we performed the same experiments as reported in Ref. 16. The experiments were performed with the incident beam parallel to a (the rung direction). We sum the data collected in the horizontal detector banks at each incident energy, thereby integrating over approximately one Brillouin zone in Q_{\parallel} . In Fig. 3 the data collected with incident energies of 150, 300, 500, and 600 meV are shown. The insets illustrate the range of (Q, ω) space over which the integration is made and its relationship to the dispersion relation. The data are analyzed with a method similar to that in Ref. 16. The scattering function and the dispersion relation are assumed as in Ref. 16. In the calculation the misalignment of the four crystals is taken into account. The function was then convoluted with the instrumental resolution function and fitted to the data collected with incident energies with 150, 300, 500, and 600 meV simultaneously. The fits to the four data sets are shown in Fig. 3, and yielded the band minimum (spin gap) of 30.5 ± 5 meV and the band maximum of 191 ± 5 meV. The model fitting in Fig. 3 is not as good as in Ref. 16 because of smaller sample mass and mostly because of a misalignment of the crystals, which cannot be fully corrected with the model function. However, the upper limit of the scattering is observable at ~ 200 meV particularly in the 300 meV and 500 meV data as shown in Fig. 3, suggesting that the band maximum should be similar to the fitted value.

B. $\omega-q$ dispersion

The dispersion data $\omega(Q)$ as obtained from the peak positions are shown in Fig. 4. The signals at 30–60 meV originate from the bottom of the excitation band in the first Brillouin zone and those at 100–170 meV from the excitations in the second zone. The minima of the dispersion are expected at $Q \sim 0.8$ and $\sim 2.4 \text{ \AA}^{-1}$, which corresponds to the π and 3π points, respectively. As shown in Fig. 5, all the experimental points are reduced to a single Brillouin zone. These points constitute a dispersion curve for the lowest energy excitation.

C. Exchange interactions between copper ions

The standard analysis of experimental data for spin ladders uses the two parameters J_{leg} and J_{rung} only, assuming the simplest symmetric structure of the two legged ladder. For this model we have calculated the dispersion of the lowest triplet excitation using the Lanczos method for ladders with 12 rungs (i.e., 24 spins) and periodic boundary conditions. Although this ladder is of limited length and allows us to calculate the energy of the excited triplet for a limited number of Q values only, the results are reliable owing to the short correlation length of the spin ladder (about three rungs).

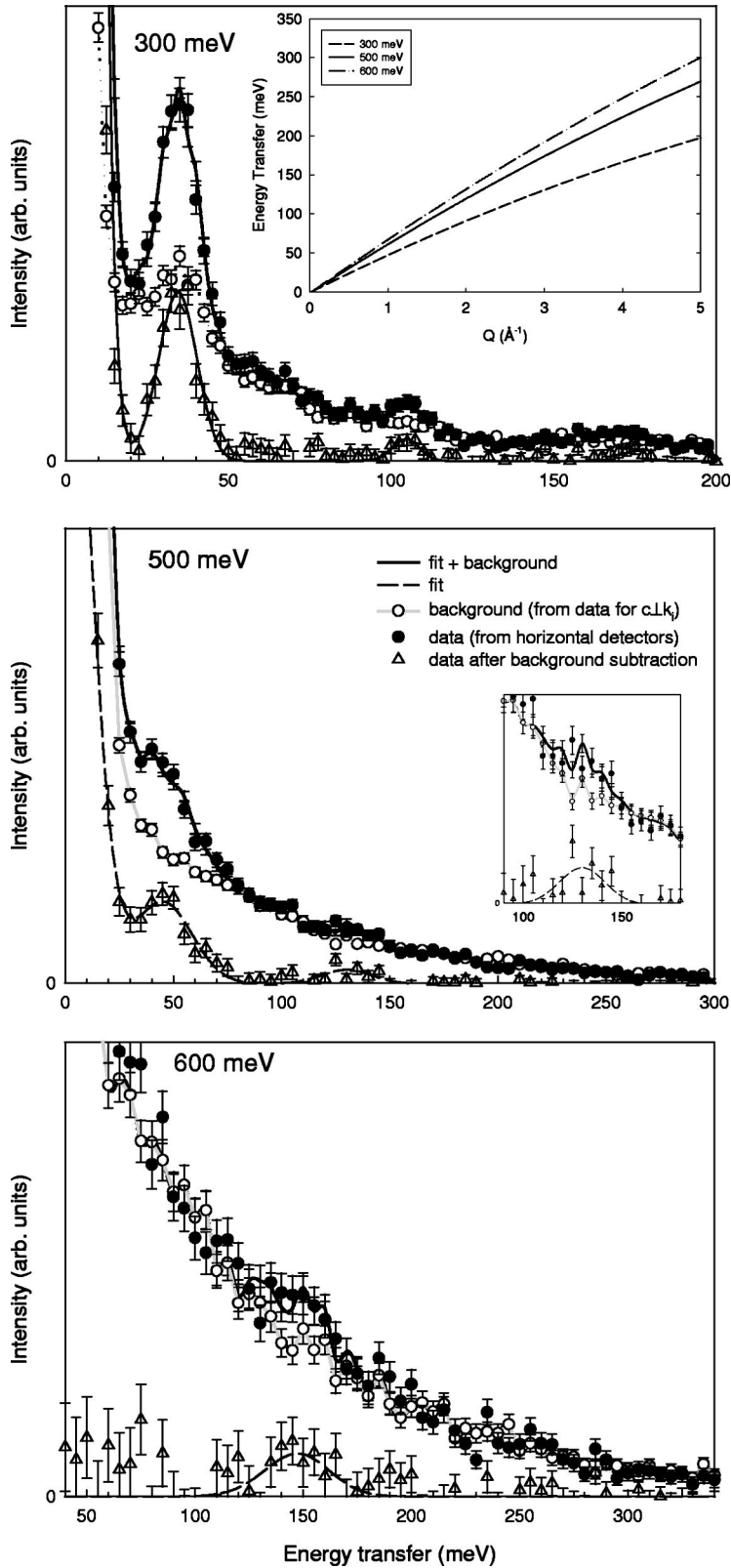


FIG. 2. Inelastic neutron scans of $\text{La}_6\text{Ca}_8\text{Cu}_{24}\text{O}_{41}$ measured at $T=20$ K with incident neutron energies of 300, 500, and 600 meV. The filled and open circles represent the raw spectrum and the background signal, respectively. The open triangles represent the spectrum after subtracting the background. The gray curves are guides to the eye. The broken curves are the results of fits to a convolution of the resolution function with Gaussians. The solid curves are the fitted value added to the background. The inset in the top figure shows the scan loci in $\omega-Q$ space. The inset in the middle figure shows neutron signals around 130 meV measured with an incident neutron energy of 500 meV.

With J_{rung} and J_{leg} as only exchange parameters we obtained the reasonable fit to our data for $J_{\text{rung}}=53$ meV and $J_{\text{leg}}=106$ meV, corresponding to $J_{\text{leg}}/J_{\text{rung}}=2$, as shown in Fig. 5. It is noted that these parameters are determined so that the minimum and maximum of the triplet excitation band, which are determined as shown in Sec. III A, are reproduced. These values are in good agreement with those obtained before;¹⁶ they are, however, not consistent (i) with

the expectation from a geometrical consideration that the Cu-O-Cu exchange on legs and rungs should be approximately equal (due to identical exchange paths and approximately equal distances and also in analogy to 2D materials such as La_2CuO_4) and (ii) with the results of an exact diagonalization calculation for the electronic state of cuprates performed by Mizuno *et al.*,²² which gives $J_{\text{rung}}\sim 150$ meV and $J_{\text{leg}}\sim 170$ meV, corresponding to $J_{\text{leg}}/J_{\text{rung}}=1.1$.

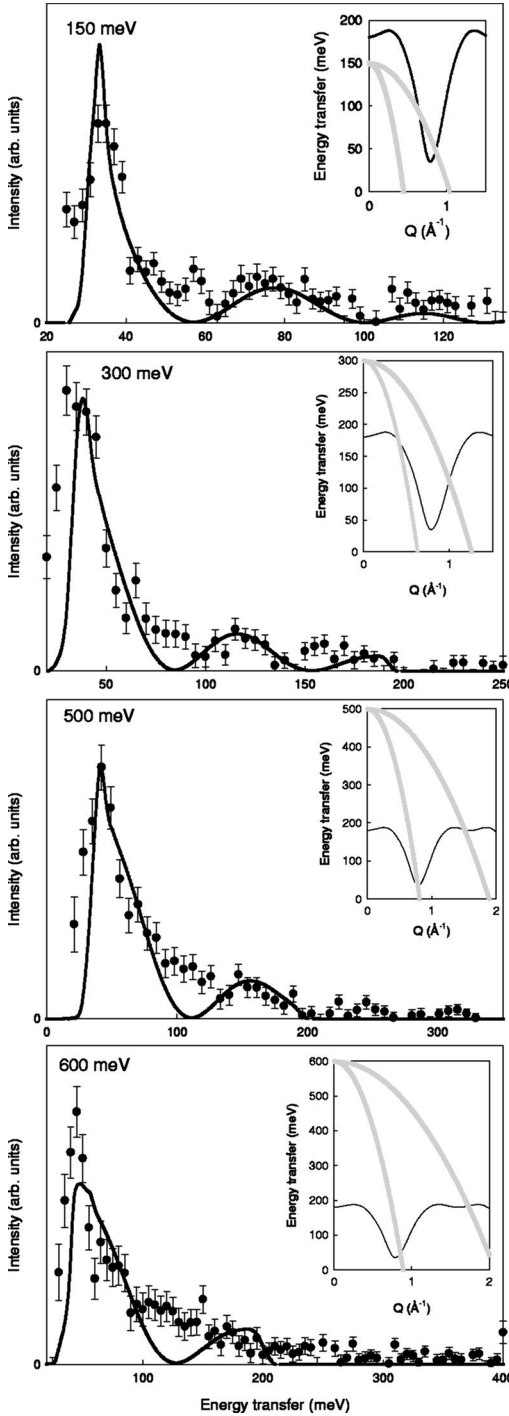


FIG. 3. Scattering integrated over the low angle bank with incident energies 150, 300, 500, and 600 meV. The solid lines are the results of fits described in the text. The insets show the relationship between the dispersion relation and the portions of (Q, ω) space over which the scattering was integrated.

We, therefore, considered whether or not the introduction of additional exchange interactions gives a fit to our data with comparable accuracy and concomitantly is consistent with the expectation $J_{\text{ring}} \approx J_{\text{leg}}$. We first calculated the dispersion for the fixed value $J_{\text{leg}}/J_{\text{ring}} = 1$ with an additional next-nearest-neighbor exchange J_{diag} (exchange across diagonals of the basic ladder plaquette). The reasonable fit to our dispersion data was obtained for $J_{\text{diag}}/J_{\text{ring}} \sim -0.4$. This

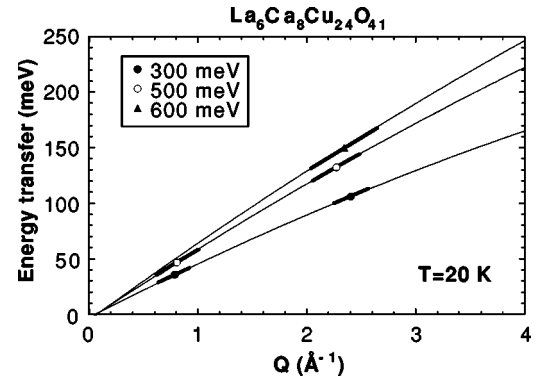


FIG. 4. $\omega-Q$ dispersion relation for the two-leg spin ladder in $\text{La}_6\text{Ca}_8\text{Cu}_{24}\text{O}_{41}$. The various symbols represent the positions where magnetic excitation peaks are observed. The thin and thick lines represent the scan loci and the error bars of the observed data.

possibility, however, has to be discarded since it is incompatible with the theoretical result^{23–25} that J_{diag} is antiferromagnetic.

Next, we calculated the dispersion with an additional ring exchange J_{ring} . A possibility of the presence of a four-spin exchange interaction of the form

$$H_{\text{ring}} = 2J_{\text{ring}}[(\mathbf{S}_1 \cdot \mathbf{S}_2)(\mathbf{S}_3 \cdot \mathbf{S}_4) + (\mathbf{S}_1 \cdot \mathbf{S}_4)(\mathbf{S}_2 \cdot \mathbf{S}_3) - (\mathbf{S}_1 \cdot \mathbf{S}_3)(\mathbf{S}_2 \cdot \mathbf{S}_4)], \quad (1)$$

which for $S = \frac{1}{2}$ describes ring exchange around a plaquette formed by the four spins \mathbf{S}_1 , \mathbf{S}_2 , \mathbf{S}_3 , and \mathbf{S}_4 was recently proposed by Brehmer *et al.*²⁶ It was shown that the ring exchange reduces the gap energy at $Q = \pi$ considerably, thereby requires larger values for J_{ring} and J_{leg} . The four-spin terms in Eq. (1) actually are the simplest ones present in an $S = \frac{1}{2}$ ladder, since the best known four-spin term, the biquadratic exchange $J_{\text{biq}}(\mathbf{S}_1 \cdot \mathbf{S}_2)^2$, reduces to two-spin exchange interactions for $S = \frac{1}{2}$ and is not an independent op-

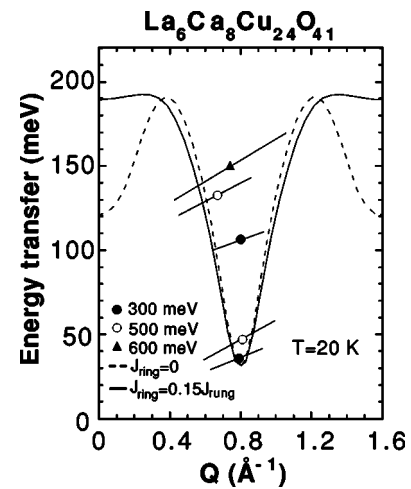


FIG. 5. $\omega-Q$ dispersion relation reduced to a single Brillouin zone for the two-leg spin ladder in $\text{La}_6\text{Ca}_8\text{Cu}_{24}\text{O}_{41}$. The broken curve represents the theoretical one with $J_{\text{leg}} = 106$ meV and $J_{\text{ring}} = 53$ meV. The solid curve represents the theoretical one with $J_{\text{leg}} = J_{\text{ring}} = 110$ meV and $J_{\text{ring}} = 16.5$ meV. These theoretical curves are drawn through the points calculated for $Q = (n/6)\pi$ ($n = 0, 1, \dots, 6$).

erator. We calculated the dispersion, again with the fixed value $J_{\text{leg}}/J_{\text{rung}} = 1$ for nonzero J_{ring} . The solid curve in Fig. 5 shows the theoretical one with $J_{\text{rung}} = 110$ meV, $J_{\text{leg}} = 110$ meV, and $J_{\text{ring}} = 16.5$ meV.

These results suggest that a moderate amount of ring exchange around the basic ladder plaquettes (about 15% of the main Cu-O-Cu bilinear exchange) should be included into the Hamiltonian of the two-leg ladder. We emphasize, however, that this conclusion is not based on a difference in quality between the two calculations presented in Fig. 5 (to the contrary: the two calculations presented in Fig. 5 are essentially of same quality) but on the following arguments:

(i) The result obtained including J_{ring} is consistent with the geometrical expectation $J_{\text{rung}} \approx J_{\text{leg}}$ which is also found in the exact diagonalization calculation.

(ii) The values for J_{rung} and J_{leg} found in this way are close to those obtained in La_2CuO_4 ($J \sim 130\text{--}190$ meV),^{23–25} in which the Cu-O-Cu exchange paths are similar to those in the ladder compound.

(iii) The value for J_{ring} obtained here is close to the theoretical one $J_{\text{ring}} = 19$ meV predicted for La_2CuO_4 .²⁴ Very recently, J_{ring} and J_{diag} in the Cu_2O_3 ladder have been obtained from the exact diagonalization calculation.²⁷ J_{ring} and J_{diag} are calculated to be 18 meV and 3 meV, respectively, which is quite consistent with our experimental results. It is noted that J_{ring} has been considered in the CuO_2 planes by Lorenzana *et al.*²⁸ very recently in order to interpret the optical absorption results in La_2CuO_4 , $\text{YBa}_2\text{Cu}_3\text{O}_6$, and $\text{Sr}_2\text{CuO}_2\text{Cl}_2$. They claim that J_{ring} should be finite and have a value of $\sim 0.3J$, where J is the interaction between nearest-neighbor copper ions in the CuO_2 plane.

The ratio $J_{\text{leg}}/J_{\text{rung}} \sim 1$, at a glance, does not seem to be consistent with the recent result of Imai *et al.* who obtained $J_{\text{leg}}/J_{\text{rung}} \sim 2$ for both $\text{La}_6\text{Ca}_8\text{Cu}_{24}\text{O}_{41}$ and $\text{Sr}_{14}\text{Cu}_{24}\text{O}_{41}$ from ^{17}O NMR measurements.¹⁵ The actual quantity they measured is the spin density at the two oxygen sites.¹⁵ If one assumes J_{leg} and J_{rung} only, one gets $J_{\text{leg}}/J_{\text{rung}} \sim 2$ from the

experiment. So, there is no contradiction between the NMR and the present experiments. The absolute values of J_{leg} and J_{rung} determined from the present study are still considerably smaller than the theoretical ones.²² One reason for this discrepancy would be that the calculation was made on SrCu_2O_3 which has a similar ladder structure as $\text{La}_6\text{Ca}_8\text{Cu}_{24}\text{O}_{41}$. A detailed calculation of the exchange constants in $\text{La}_6\text{Ca}_8\text{Cu}_{24}\text{O}_{41}$ using the parameters appropriate for this material will give a better result.

IV. SUMMARY

Using a pulsed neutron source we have been able to observe inelastic signals up to ~ 200 meV from the ladders of $\text{La}_6\text{Ca}_8\text{Cu}_{24}\text{O}_{41}$. These signals constitute the magnon branch for the lowest triplet excitation. A fit to a theory including a coupling along the leg (J_{leg}) and rung (J_{rung}) alone gives values which are not compatible with the expectation from a geometrical consideration and the theoretical prediction $J_{\text{leg}} \approx J_{\text{rung}}$. Therefore, we introduced a four-spin exchange interaction (J_{ring}) in addition to J_{leg} and J_{rung} . A reasonable fit is obtained with $J_{\text{leg}} = J_{\text{rung}} = 110$ meV, and $J_{\text{ring}} = 16.5$ meV. In a future experiment, it would be interesting to measure the temperature dependence of the excitation spectrum. The temperature dependence of the intensity at $Q = \pi$ is predicted to exhibit a peak at a temperature below that corresponding to spin gap.²⁹

ACKNOWLEDGMENTS

We would like to thank S. Maekawa, Y. Mizuno, G. Shirane, and T. Tohyama for stimulating discussions. This work was carried out as part of the RIKEN-CCLRC Collaborative Studies in Neutron Science. The work done in Japan was supported in part by a Grant-in-Aid for Scientific Research from the Japanese Ministry of Education, Science, Sports, and Culture.

*Present address: Advanced Science Research Center, Japan Atomic Energy Research Institute, Tokai, Ibaraki 319-1195, Japan.

¹For a review, see E. Dagotto and T. M. Rice, *Science* **271**, 618 (1996).

²E. Dagotto, J. Riera, and D. Scalapino, *Phys. Rev. B* **45**, 5744 (1992).

³T. M. Rice, S. Gopalan, and M. Sigrist, *Europhys. Lett.* **23**, 445 (1993).

⁴T. Barnes, E. Dagotto, J. Riera, and E. S. Swanson, *Phys. Rev. B* **47**, 3196 (1993).

⁵S. Gopalan, T. M. Rice, and M. Sigrist, *Phys. Rev. B* **49**, 8901 (1994).

⁶T. Barnes and J. Riera, *Phys. Rev. B* **50**, 6817 (1994).

⁷M. Reigrotzki, H. Tsunetsugu, and T. M. Rice, *J. Phys.: Condens. Matter* **6**, 9235 (1994).

⁸J. Oitmaa, R. R. P. Singh, and Z. Weihong, *Phys. Rev. B* **54**, 1009 (1996).

⁹S. R. White, R. M. Noack, and D. J. Scalapino, *Phys. Rev. Lett.* **73**, 886 (1994).

¹⁰E. M. McCarron III, M. A. Subramanian, J. C. Calabrese, and R. L. Harlow, *Mater. Res. Bull.* **23**, 1355 (1988).

¹¹T. Siegrist, L. F. Schneemeyer, S. A. Sunshine, J. V. Waszczak,

and R. S. Roth, *Mater. Res. Bull.* **23**, 1429 (1988).

¹²K. Kumagai, S. Tsuji, M. Kato, and Y. Koike, *Phys. Rev. Lett.* **78**, 1992 (1997).

¹³M. Takigawa, N. Motoyama, H. Eisaki, and S. Uchida, *Phys. Rev. B* **57**, 1124 (1998).

¹⁴K. Magishi, S. Matsumoto, Y. Kitaoka, K. Ishida, K. Asayama, M. Uehara, T. Nagata, and J. Akimitsu, *Phys. Rev. B* **57**, 11 533 (1998).

¹⁵T. Imai, K. R. Thurber, K. M. Shen, A. W. Hunt, and F. C. Chou, *Phys. Rev. Lett.* **81**, 220 (1998).

¹⁶R. S. Eccleston, M. Uehara, J. Akimitsu, H. Eisaki, N. Motoyama, and S. Uchida, *Phys. Rev. Lett.* **81**, 1702 (1998).

¹⁷S. A. Carter, B. Batlogg, R. J. Cava, J. J. Krajewski, W. F. Peck, Jr., and T. M. Rice, *Phys. Rev. Lett.* **77**, 1378 (1996).

¹⁸M. Kato, K. Shiotani, and Y. Koike, *Physica C* **258**, 284 (1996).

¹⁹Y. Mizuno, T. Tohyama, and S. Maekawa, *J. Phys. Soc. Jpn.* **66**, 937 (1997).

²⁰T. Osafune, N. Motoyama, H. Eisaki, and S. Uchida, *Phys. Rev. Lett.* **78**, 1980 (1997).

²¹M. Matsuda, K. Katsumata, T. Yokoo, S. M. Shapiro, and G. Shirane, *Phys. Rev. B* **54**, R15 626 (1996).

²²Y. Mizuno, T. Tohyama, and S. Maekawa, *Phys. Rev. B* **58**, R14 713 (1998).

- ²³J. F. Annett, R. M. Martin, A. K. McMahan, and S. Satpathy, *Phys. Rev. B* **40**, 2620 (1989).
- ²⁴H. J. Schmidt and Y. Kuramoto, *Physica C* **167**, 263 (1990).
- ²⁵T. Tohyama and S. Maekawa, *J. Phys. Soc. Jpn.* **59**, 1760 (1990).
- ²⁶S. Brehmer, H.-J. Mikeska, M. Müller, N. Nagaosa, and S. Uchida, *Phys. Rev. B* **60**, 329 (1999).
- ²⁷Y. Mizuno, T. Tohyama, and S. Maekawa, *J. Low Temp. Phys.* **117**, 389 (1999).
- ²⁸J. Lorenzana, J. Eroles, and S. Sorella, *Phys. Rev. Lett.* **83**, 5122 (1999).
- ²⁹M. Greven, R. J. Birgeneau, and U.-J. Wiese, *Phys. Rev. Lett.* **77**, 1865 (1996).